Transverse surface modes in ferromagnets: Coupled $\vec{M}$ and $\vec{m}$

Chen Sun[1,*] and Wayne M. Saslow[2,†]
[1]*Department of Physics, Brown University, Providence, Rhode Island, 02912, USA*
[2]*Department of Physics, Texas A&M University, College Station, Texas, 77843-4242, USA*

(Received 9 January 2019; published 29 March 2019)

Ferromagnets, when out of equilibrium, have two sets of transverse variables: the tipped magnetization $d\vec{M}$, arising from the changed eigenstate, and the transverse component of the spin accumulation $\vec{m}$, arising from the nonequilibrium spin distribution function (where $\vec{m} = \vec{0}$ in equilibrium). For conductors, $\vec{m}$ is due a nonequilibrium distribution of electrons near the Fermi surface; for insulators, $\vec{m}$ is due to a nonequilibrium distribution of magnons. Applying irreversible thermodynamics to these four transverse degrees of freedom gives, in the small-amplitude limit, four static transverse surface modes (evanescent modes) of $d\vec{M}$ and $\vec{m}$, which couple both by uniform mean-field exchange λ and by the recently noted mutual decay rate τ_{mM}^{-1}. As prototype ferromagnets we consider static, pairwise degenerate modes for the insulator yttrium iron garnet (YIG) and the conductor permalloy (Py). YIG has much longer longitudinal and transverse decay lengths than Py. Numerical studies are made of the eigenmodes (ratio of $d\vec{M}$ to $\vec{m}$) and of the real and imaginary parts of the two eigenwave vectors; they reveal much about the dependence of the modes on field H, λ, χ_f (transverse spin accumulation susceptibility), $\chi_\perp$ (transverse magnetization susceptibility), and τ_{mM}. For example, when χ_f is very small, as expected at low temperatures, both transverse modes are dominated by $d\vec{M}$. The transverse decay lengths typically are much shorter than the longitudinal (spin-flip) decay length, largely because they are subject to exchange-field precession. Thus, ultrathin samples can give a full transverse response (such as transverse "magnon-mediated" charge current "drag"), but thick samples can give neither longitudinal nor transverse response. With amplitudes determined by the boundary conditions on $\vec{m}$ and $\vec{M}$, these modes permit the interior of the ferromagnet to respond in a spatially varying fashion. The six transverse boundary conditions at an N/F interface are briefly discussed. For small enough sample thicknesses, relative to the transverse decay lengths, there should be a transverse "magnon drag" phenomenon, both for conductors and insulators.

DOI: 10.1103/PhysRevB.99.104435

I. INTRODUCTION

Johnson and Silsbee developed the thermodynamics of a conducting ferromagnet of moment $\vec{M}$ slightly out of equilibrium [1]. In an Appendix they used irreversible thermodynamics to study the static spin transfer of longitudinal spin current from a conducting ferromagnet to a paramagnetic conductor. They found decaying modes (i.e., surface modes, also known as *evanescent modes*) of *longitudinal* spin in both materials [2]. Then, for a fixed charge current, they employed charge current continuity and two spin current boundary conditions at the interface to find the two unknown mode amplitudes for the longitudinal spin current in each material.

One spin boundary condition was continuity of the longitudinal spin current $\vec{j}_{s,L}$. The other, from irreversible thermodynamics, was that $\vec{j}_{s,L}$ across the interface is proportional to the difference across the interface in the longitudinal spin chemical potential $\vec{\mu}_L$ (they employed an effective field H^* rather than $\vec{\mu}_L$). Two previous works, not employing irreversible thermodynamics boundary conditions, had taken different, phenomenological, boundary conditions [3,4]. The associated nonequilibrium magnetization is called the longitudinal *spin accumulation*, and is equivalent to dM [5].

Reference [1] is relevant to giant magnetoresistance [5–7] as a dc read mechanism for magnetic data. Slonczewski proposed a dc write mechanism for magnetic data, emphasizing *transverse* spin transfer from normal to ferromagnet and from ferromagnet to normal [8]. It involved five materials: two normal contacts we call NL and NR (at the left and right) sandwiching a set of F1/N/F2 layers, for *noncollinear* equilibrium magnetizations $\vec{M}_1$ and $\vec{M}_2$. (When thick enough, the layer of N decouples F1 and F2 [9].) With dc current entering from the left, at the NL/F1 interface the problem was basically that studied by Johnson and Silsbee. However, some of the spin-polarized current crossing the F1/N interface and then entering F2 is polarized normal to the magnetization in F2. This leads to a transverse *spin transfer* that for large amplitudes was predicted to change the direction of the magnetization in F2. The predicted change in direction of the magnetization was shortly observed [10,11].

This work studies only the small-amplitude, linearized, dc response to transverse spin transfer. It employs the $\vec{M}$-$\vec{m}$ model for the transverse response of a ferromagnet, for which the variable $d\vec{M}$ represents the tipped magnetic quantization axis, and $\vec{m}$ represents the effect of a nonequilibrium distribution of excitations. Since dM is the longitudinal component of $\vec{m}$, we have $dM = \vec{M} \cdot \vec{m}$. Each transverse magnetic variable

*chen.sun.whu@gmail.com
†wsaslow@tamu.edu

is constrained by boundary conditions, associated either with magnetics or spin transfer. The transverse degrees of freedom couple, yielding transverse modes with decay lengths that for yttrium iron garnet (YIG) we estimate to be in the 2–10 nm range.

Section II gives a theoretical review. Section III considers the nonequilibrium transverse response of conducting and insulating ferromagnets. For conductors it uses Fermi surface related arguments to explain how it arises. It also discusses criticisms of the related theory of Silsbee, Janossy, and Monod [12], which has mathematically equivalent transverse variables but a different physical picture. Section IV considers the mathematics of the transverse eigenvalues and eigenmodes (specified by wave vectors k) for a conducting ferromagnet when anisotropy effects are small. In the absence of electric current there is no essential difference between conducting and nonconducting ferromagnets [13], so the considerations of this section also apply to insulators.

Section V assembles material parameters for both the conductor permalloy (Py) and the insulator YIG. Section VI considers the general interpretation of the numerics that follow. Section VII considers mode details for YIG, including the dependence of the transverse eigenvectors and eigenwave vectors and normal modes on applied field H, the $\vec{M}$-$\vec{m}$ uniform exchange constant λ, the transverse spin accumulation susceptibility χ_f, and the transverse magnetization susceptibility $\chi_\perp$. Section VIII considers the corresponding mode details for Py. Section IX, using the fact that typically the longitudinal decay length is much longer than either transverse decay length, discusses how the results of transverse spin response experiments (using very thin samples) might change on going to thicker samples. In addition to the "magnon-mediated" electric current "drag" effect for spin accumulation along the host magnetization [14–17], for thin enough samples the analogous effect may be observable for spin accumulation transverse to the host magnetization.

Section X considers additional implications of this work, Sec. XI provides a summary and conclusions. Appendix considers the effect on the surface mode wave vectors of the so-far unstudied cross decay between $\vec{M}$ and $\vec{m}$.

A considerable amount of current work emphasizes ferromagnetic insulators like YIG. These support magnons (magnonics), and although not eliminating the heating effects of spin currents [18], do eliminate the heating effects of charge currents [19,20]. This study of ferromagnetic insulators takes us from the short surface mode penetration depths of conductors to the much larger surface mode penetration depths of insulators, and should facilitate observation of related surface effects.

In particular, in Sec. VII this work predicts a new effect, i.e., the transverse version of the (longitudinal) "magnon drag" effect predicted by Zhang and Zhang, and observed by multiple groups [14]. It involves the shorter transverse decay lengths associated with the coupled modes of $\vec{m}$ and $d\vec{M}$, and thus will require different experimental geometries from those for which the (longitudinal) "magnon drag" was observed (see Fig. 8). More generally, the $\vec{M}$-$\vec{m}$ formalism should be applicable to all transport problems involving the transverse response of ferromagnets.

II. THEORETICAL REVIEW

In addition to predicting spin transfer, Ref. [8] argued that the spin current, on entering F2, almost immediately in space redefines the longitudinal direction in F2. As a consequence, in this picture no nonequilibrium transverse component of the magnetization is permitted. It also yields a transverse response in the ferromagnet that is completely independent of the boundary conditions on $\vec{M}$ and $\vec{m}$.

This influenced the Keldysh-based theory of Brataas, Nazarov, and Bauer, for F/N interface spin transfer [21], which employed thermodynamic variables including the spin chemical potential, as in irreversible thermodynamics. By literally accepting the physical picture of Ref. [8], no nonequilibrium transverse spin component could appear in F, although it could appear in N. This left the theory unsymmetrical: spin currents could be driven from N to F but not from F to N.

This simplification is not unlike the classical picture where a conductor screens an electric field immediately at the interface, thus neglecting the quantum-mechanical Friedel oscillations that occur near the interface. Moreover, for conducting nonmagnetic-magnetic interfaces detailed quantum-mechanical studies show, in addition to spin-dependent reflection and transmission, Fermi wave-vector-dependent spin oscillations extending into the ferromagnet [22]. As a consequence, the physical picture of Ref. [8], although clearly and correctly predicting the qualitative phenomenon of spin transfer, is an approximation. We believe it is especially valid for very thin samples, where bulk decay and precession processes near the surface have little effect. This work is directed toward thicker samples.

Not accepting the physical picture of Ref. [8], Zhang, Levy, and Fert [23] adapted the *s-d* model of a ferromagnet to spin transfer [24,25]. This model employs magnetization $\vec{M}_d$ (like the usual magnetization $\vec{M}$) for immobile magnetic d electrons, and $\vec{M}_s$ (like the spin accumulation $\vec{m}$) for mobile but polarizable s electrons [5]. For specific boundary conditions, this work studied the adjustment of the ferromagnet when a spin-polarized current entered it.

In fact, work on F $\rightleftarrows$ N flow using the *s-d* model had been done previously. Silsbee, Janossy, and Monod observed excess damping in FMR for an F (permalloy, Fe, Ni) that was adjacent to a layer of N (Cu) [12]. To explain this, they developed an irreversible-thermodynamics-inspired theory that permitted a transverse nonequilibrium response for an F, first order in the ac field. Thus, it was symmetrical relative to interfacial spin currents to and from F and N. This phenomenon of spin current driven from F to N was named *spin pumping* [26]. Currently, the term spin pumping is also employed to denote the second-order, dc spin current (detected by the inverse spin Hall effect), that accompanies first-order ac spin pumping.

Reference [12] considered that FMR directly drives a transverse exchange field which, through the boundary conditions on the s electrons, indirectly drives a spin current from F to N, just as in previous work by Flesner, Fredkin, and Schultz on electron spin resonance (ESR) from N1 to N2 [27]. With two transverse spin accumulation degrees of freedom in both F and N, Ref. [12] employed two boundary conditions on each component to make the problem completely defined.

Unlike this work, Ref. [12] included no additional modes coupling transverse $\vec{M}$ to transverse $\vec{m}$, and no corresponding $\vec{M}$ boundary conditions were considered. The theory of Ref. [12], when taken to second order in the driving field, yields a dc spin current proportional to the power absorbed, and therefore a dc spin Hall voltage proportional to the power absorbed.

It has been shown that the *s-d* model can be replaced by a more rigorous Fermi liquid theory based model of a conducting ferromagnet using the quantization axis $\hat{M}$ and the spin accumulation $\vec{m}$ (associated with a nonequilibrium distribution function) [28].

This work shows that a macroscopic, irreversible thermodynamics-based theory yields four surface modes, and applies to both conducting and insulating magnets [13]. By applying the boundary conditions on $\vec{M}$ and $\vec{m}$, one can determine the normal mode amplitudes and thus the transverse response of the ferromagnet within its interior.

In general, the equations of motion and boundary conditions for both $\vec{M}$ and $\vec{m}$ must be considered. This leads to two transverse components for both $\vec{M}$ and $\vec{m}$, each with distinct equations of motion, which recently have been derived in detail using irreversible thermodynamics [13]. In addition to exchange coupling, $\vec{M}$ and $\vec{m}$ also are coupled by mutual decay (cross decay), with four coupled transverse modes. Because an adjacent normal metal N has two transverse modes of its own $\vec{m}$, in transverse spin transfer from N to F there are two reflected modes in N and four transmitted modes in F.

At the microscopic level, insulating ferromagnets have spin properties that are distinct from those of conducting ferromagnets since the magnetism is due to magnons; this has led to the term *magnonics*. However, at the macroscopic level, insulating ferromagnets have spin properties that are nearly identical to those of conducting ferromagnets. In particular, they satisfy the same $\vec{M}$ and $\vec{m}$ boundary conditions [13].

III. TRANSVERSE RESPONSE: $\vec{M}$ AND $\vec{m}$

Although more recent work points to ferromagnetic insulators as more promising for spintronics applications because they have no Joule heating, the first studies of the nonequilibrium transport transverse response of ferromagnets were performed for conductors [10,11]. We therefore consider conductors first. Our purpose is to establish that this nonequilibrium transport transverse response of ferromagnets includes two sets of coupled surface modes of $\vec{M}$ and $\vec{m}$.

We first note that, for a longitudinal spin current, the spin of the excitations must be opposed to the majority spin direction, with a large increase in exchange energy. Nevertheless, longitudinal spin currents have been observed. We conclude that the necessarily large exchange energy does not inhibit the generation of longitudinal spin currents, and therefore we conclude that the much smaller exchange energy required to excite slightly tipped transverse excitations should be even less inhibited. Nevertheless, we provide a physical picture of how transverse spin accumulation can arise.

Consider a conducting ferromagnet F having majority carrier excitations above the Fermi surface, with spin slightly misaligned relative to the quantization axis $\hat{M}$ by characteristic angle θ. They have a transverse spin accumulation $\vec{m}$ of magnitude $\sim|\theta|$ but gain only an exchange energy $\sim\theta^2$ ($\vec{m}=\vec{0}$ in equilibrium). Figure 1 illustrates typical low-energy excitations that lead to a transverse spin accumulation $\vec{m}$. Just as $\vec{m}$ represents changes from equilibrium in the distribution function at fixed spin eigenstates, so $d\vec{M}$ represents changes in the spin eigenstates.

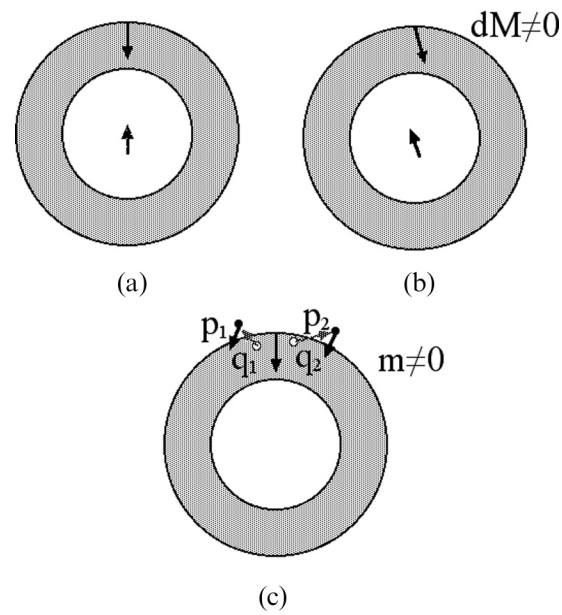

FIG. 1. Excitations above the upper magnetic Fermi sea, with thick spin vectors tilted slightly relative to majority spin direction. Part (a) represents the unrotated ground state, with vertical spin quantization axis. There are no excitations. Part (b) represents the rotated ground state, with tipped spin quantization axis, represented by $d\vec{M}\neq\vec{0}$. There are no excitations. In part (c), empty states below the Fermi sea have white circles with a dark downward arrow indicating spin polarization, and filled states above the Fermi sea have dark circles with tilted spin-polarization arrows. Thin arrows indicate transitions from below to above the Fermi sea.

Note that the longitudinal components of $d\vec{M}$ and $\vec{m}$, or dM and $\hat{M}\cdot\vec{m}$, are equivalent. Hence, there are five, not six, independent components to $\vec{M}$ and $\vec{m}$. Reference [1] employed dM, but $\hat{M}\cdot\vec{m}$ is a bit more consistent with the idea of excitations, or spin accumulation. On the other hand, the transverse magnetization has contributions both from the transverse spin accumulation $\vec{m}$ and from the tipped magnetization $\vec{M}$.

As for the longitudinal spin accumulation, each transverse component of $\vec{m}$ satisfies two boundary conditions. In addition, the two components of transverse $\vec{M}$ satisfy boundary conditions from micromagnetics, which arise from the equation of motion for $\vec{M}$ evaluated for the spins on the surface. We do not apply the boundary conditions in this work.

Although the related theory of Silsbee, Janossy, and Monod (SJM) successfully explained the line shape observed in spin pumping [12], some criticisms have been made of their theory [29], which we now address:

(i) The original form of the theory uses both localized (d) and conduction (s) spins. However, as noted above, it was later shown that Fermi liquid theory gives the equivalent two transverse variables $d\vec{M}$ (from tipping the quantization axis) and spin accumulation $\vec{m}$ (from electron excitations) [13,28].

Therefore, SJM can be reinterpreted in terms of Fermi liquid theory.

(ii) The original form of the theory does not treat magnetic insulators. However, as shown in the Appendix to Ref. [13], the same variables $d\vec{M}$ and $\vec{m}$ apply for ferromagnetic insulators, with $\vec{m}$ now due to magnon excitations.

(iii) The theory does not use microscopically defined surface transport parameters. However, the literature contained computations of the longitudinal surface spin current transport parameters [30–32]. Moreover, Ref. [21] was general enough to later yield the corresponding values for the longitudinal and transverse spin current transport parameters. Indeed, had the authors of Ref. [21] not explicitly forbidden transverse spin accumulation from the final version of their theory, then they would have obtained a theory equivalent to that of Ref. [12], with appropriate microscopically defined surface transport parameters.

Microscopically defined surface transport parameters were later employed to describe the irreversible-thermodynamic-based spin "backflow" associated with the spin accumulation in the normal material [33]. Perhaps the first surface transport theory, that of Khalatnikov for phonon heat flux [34], computed the conversion of phonon heat flux in one material to that in the adjacent material. Moreover, the more recent spin "convertance" of Zhang and Zhang computes the conversion of spin current from magnetic excitations in a conductor to spin current from magnons in an adjacent insulator [35].

We now consider the mathematical origin of the spin accumulation in conductors, with spin due to electrons, of spin $\frac{1}{2}$. It is well known that for conduction electrons the local spin density (the spin accumulation, with spin index $i = 1, 2, 3$) is proportional to

$$\tfrac{1}{2}\langle\alpha|\,\sigma^i_{\alpha\beta}\,|\beta\rangle,$$

where the $\sigma^i_{\alpha\beta}$ are the Pauli matrices with index i running from 1 to 3. The indices α and β take on the values $-\frac{1}{2}$ and $+\frac{1}{2}$, and represent only the spin part of the electron wave function. This definition applies both to the longitudinal and the transverse spin accumulation in a conductor [13,28].

The situation is very similar in insulators. Let an insulator, such as YIG (yttrium iron garnet), have effective spin S (later, we take $S = 14.5$). Then, the local spin density (again the spin accumulation, with spin index $i = 1, 2, 3$) is proportional to

$$\langle\alpha|\,S^i_{\alpha\beta}\,|\beta\rangle,$$

where the $S^i_{\alpha\beta}$ are the angular momentum matrices for spin S with with index i running from 1 to 3, and the indices α and β, which go in integer steps from $-S$ to $+S$, represent only the spin part of the electron wave function. We do not need to know the actual spin matrices $S^i_{\alpha\beta}$.

It is important to note the following: The irreversible thermodynamics mechanism for driving transverse spin currents across an interface is frequency independent; thus, it can be distinguished from the resonance frequency dependence of what has been called the "coherent" theory [26]. Moreover, the two theories have a different dependence on the spin polarization.

To be specific, the dominant term in spin current $\vec{j}_s$ crossing the interface in the coherent theory varies as $\hat{M}\times d\vec{M}/dt$ [26]. This has, for equilibrium $\vec{M}_0$ along $\hat{z}$ and an $e^{-i\omega t}$ time dependence, the form $-i\omega M\hat{z}\times(d\hat{M}_x\hat{x}+d\hat{M}_y\hat{y}) = -i\omega M(\hat{y}d\hat{M}_x-\hat{x}d\hat{M}_y)$. On the other hand, the irreversible thermodynamics forms for the spin current crossing the interface varies as $d\hat{M}=\hat{x}d\hat{M}_x+\hat{y}d\hat{M}_y$. We summarize this by writing

$$\vec{j}_{s,T}\sim -i\omega M(\hat{y}d\hat{M}_x-\hat{x}d\hat{M}_y)\quad\text{(coherent)},\tag{1}$$

$$\vec{j}_{s,T}\sim \hat{x}d\hat{M}_x+\hat{y}d\hat{M}_y\quad\text{(irreversible thermodynamics)}.\tag{2}$$

Hence, the two approaches predict different frequency and polarization dependencies. The contrast in frequency dependence is sharpest both for the dc case and for very high ac frequencies. To our knowledge, neither the resonance frequency dependence nor the polarization dependence has been studied experimentally. Note that all surface mechanisms (irreversible thermodynamics, coherent, two-magnon decay) lead to an excess damping that varies inversely with the thickness of the ferromagnet.

IV. FOUR TRANSVERSE MODES

We now calculate the eigenvalues and eigenmodes with exchange coupling between $\vec{M}$ and $\vec{m}$, assuming no transverse component of the external field, so $\vec{H}_{0\perp}=0$. We take uniform equilibrium magnetization $\vec{M}_0$, and recall that $\vec{m}=\vec{0}$ in equilibrium.

A. Model

$\vec{M}$ and $\vec{m}$ couple both in phase by a uniform exchange constant λ, and by cross decay subject to an Onsager condition. In addition, both $\vec{M}$ and $\vec{m}$ precess in any external field and/or demagnetization field. Both also are subject to decay to the lattice ($\vec{M}$ by Landau-Lifshitz damping and $\vec{m}$ by spin flip). Finally, $\vec{M}$ is subject to a nonuniform exchange field (with constant A), and $\vec{m}$ (but not $\vec{M}$) is subject to diffusion. Symmetry permits a nonuniform exchange field $\nabla^2\vec{m}$ for $\vec{m}$, and nonuniform cross-coupling fields, which for simplicity we ignore.

B. Net magnetization

The total magnetization $\vec{\mathcal{M}}$ is given by

$$\vec{\mathcal{M}}=\vec{M}+\vec{m}.\tag{3}$$

We use SI units, so

$$\vec{B}=\mu_0(\vec{H}+\vec{\mathcal{M}})\tag{4}$$

is in tesla and $\vec{H}$ and $\vec{\mathcal{M}}$ are in A/m. For the static case with translational symmetry, we show below that $\vec{H}$ is proportional to the appropriate component of the magnetization $\vec{\mathcal{M}}$. A more general treatment, needed to solve the full boundary value problem, gives the field $\vec{H}$ its own dynamics [36–38]. In what follows, since we restrict ourselves to the transverse response, we may use $\vec{M}_\perp$ for $d\vec{M}$.

C. $\vec{M}_\perp$ and $\vec{m}_\perp$

Associated with $\vec{M}_\perp$ is an effective field $\vec{H}^*_\perp$ that is zero in local equilibrium [13]. We take an exchange energy $\varepsilon_{ex}=-\mu_0\lambda\vec{M}\cdot\vec{m}$, where the dimensionless constant λ is associated

with the term that determines the Curie temperature in simple mean-field theory. We also take the parameter A to be associated with nonuniform exchange (exchange stiffness). Then,

$$\vec{H}_\perp^* = \left(\vec{H} + \lambda\vec{m} + \frac{2A}{\mu_0 M}\nabla^2\hat{M}\right)_\perp - \frac{H}{M}\vec{M}_\perp \equiv -\frac{H}{M}\delta\vec{M}_\perp; \tag{5}$$

in local equilibrium we have $\vec{H}_\perp^* = \vec{0}$, which determines $\vec{M}_\perp$. In uniform equilibrium, if the field $\vec{H}$ rotates then $\vec{M}$ rotates, giving a transverse magnetization susceptibility

$$\chi_\perp \equiv \frac{M}{H}. \tag{6}$$

It is helpful to rewrite (5) as

$$\delta\vec{M}_\perp = -\chi_\perp\vec{H}_\perp^* = \vec{M}_\perp - \chi_\perp\left(\vec{H} + \lambda\vec{m} + \frac{2A}{\mu_0 M}\nabla^2\hat{M}\right)_\perp, \tag{7}$$

so $\delta\vec{M}_\perp = \vec{0}$ in local equilibrium [39–41]. When the system is driven with wave vector k, as e^{ikz}, so $\nabla^2 \to -k^2$, it is convenient to employ the nonuniform exchange wave vector k_A:

$$k_A = \sqrt{\frac{\mu_0 MH}{2A}}. \tag{8}$$

Then, (7) may be rewritten as

$$\delta\vec{M}_\perp = \vec{M}_\perp\left(1 + \frac{k^2}{k_A^2}\right) - \chi_\perp(\vec{H} + \lambda\vec{m})_\perp. \tag{9}$$

We now turn to the transverse spin accumulation $\vec{m}_\perp$. Associated with $\vec{m}_\perp$ is an effective field $\vec{h}_\perp^*$ that is zero in local equilibrium [13]. With χ_f the transverse component of the ferromagnet's spin accumulation susceptibility, $\vec{h}_\perp^*$ is given by [13]

$$\vec{h}_\perp^* = \left(\vec{H} + \lambda\vec{M} - \frac{\vec{m}}{\chi_f}\right)_\perp = -\frac{\delta\vec{m}_\perp}{\chi_f}, \tag{10}$$

so that in local equilibrium $\vec{h}_\perp^* = 0$ and $\delta\vec{m}_\perp = \vec{0}$. It is helpful to rewrite (10) as

$$\delta\vec{m}_\perp = \vec{m}_\perp - \chi_f(\vec{H} + \lambda\vec{M})_\perp. \tag{11}$$

We interpret $\delta\vec{m}_\perp$ as the deviation of $\vec{m}_\perp$ from instantaneous local equilibrium [39–41].

In terms of spin chemical potential $\vec{\mu}_s$ the relation $\vec{\mu}_s = (\gamma\hbar/2)\vec{h}^*$ holds [13]. Note that the spin chemical potential $\vec{\mu}_s$ is distinct from the spin accumulation $\vec{m}$, although for paramagnets in zero external field they are proportional. In what follows, it is useful to define two frequencies:

$$\omega_H \equiv \gamma\mu_0 H, \tag{12}$$

$$\omega_X \equiv \gamma\mu_0 h_\parallel^* = \omega_H + \gamma\mu_0\lambda M \approx \gamma\mu_0\lambda M. \tag{13}$$

D. Equations of motion: Degenerate transverse directions

We now write the equations of motion for $\vec{M}_\perp$ and $\vec{m}_\perp$, and then comment on various new terms that appear in Ref. [13]. For simplicity, we consider the two transverse directions as equivalent, so any anisotropy (which in practice we neglect) is uniform in the transverse plane. We take the equilibrium magnetization $\vec{M}_0$ to be along $\hat{z}$.

From Ref. [13], $\vec{M}_\perp$ and $\vec{m}_\perp$ have coupled equations of motion given by

$$\partial_t\vec{M}_\perp = \omega_H\hat{M}\times\delta\vec{M}_\perp - \frac{1}{\tau_M}\delta\vec{M}_\perp + \frac{1}{\tau_{mM}}\delta\vec{m}_\perp, \tag{14}$$

$$\partial_t\vec{m}_\perp = -\omega_X\vec{m}_\perp\times\hat{M} + D_f\nabla^2\delta\vec{m}_\perp - \frac{L_R}{\chi_f}\hat{M}\times\nabla^2\delta\vec{m}_\perp - \frac{1}{\tau_f}\delta\vec{m}_\perp + \frac{1}{\tau_{Mm}}\delta\vec{M}_\perp. \tag{15}$$

Here, with α the dimensionless Gilbert constant (the spin analog of the Q factor for a linear oscillator),

$$\frac{1}{\tau_M} = \alpha\omega_H \equiv \frac{1}{\tau_{ML}} + \frac{1}{\tau_{Mm}}, \tag{16}$$

$$\frac{1}{\tau_f} \equiv \frac{1}{\tau_{mL}} + \frac{1}{\tau_{mM}}. \tag{17}$$

The constant L_R [13] represents a stiffness for $\vec{m}_\perp$ (just as the constant A represents a stiffness for $\vec{M}_\perp$); for simplicity our numerical calculations take $L_R = 0$. There also is a transverse spin diffusion constant D_f, and

$\tau_M^{-1} = \alpha\omega_H$ (α is the dimensionless Gilbert constant); τ_{ML}^{-1} gives the decay rate of $\vec{M}_\perp$ to the lattice; τ_{mL}^{-1} gives the decay rate of $\vec{m}_\perp$ to the lattice; τ_{Mm}^{-1} gives the decay rate of $\vec{M}_\perp$ to $\vec{m}_\perp$; and τ_{mM}^{-1} gives the decay rate of $\vec{m}_\perp$ to $\vec{M}_\perp$. The last two satisfy the Onsager relation

$$\frac{\chi_\perp}{\tau_{Mm}} = \frac{\chi_f}{\tau_{mM}}. \tag{18}$$

Since we expect that $\chi_\perp \gg \chi_f$, by the above Onsager relation we thus expect $\tau_{Mm} \gg \tau_{mM}$. Hence, we expect that $\vec{M}$ decays much less quickly to $\vec{m}$ than vice versa. Both τ_{Mm}^{-1} and τ_{mM}^{-1} were introduced in Ref. [13]. However, in the s-d model of Hasegawa and in related models there is a long history of such cross decay [24,25].

In applying Maxwell's divergence equation for $\vec{B}$,

$$0 = \vec{\nabla}\cdot\vec{B} = \mu_0\vec{\nabla}\cdot(\vec{H} + \vec{\mathcal{M}}), \tag{19}$$

we consider geometries where there is no significant variation transverse to $\vec{M}_0$ (along $\hat{z}$) and (to lowest order) no variation in the longitudinal magnetization. For an e^{ikz} variation, (19) is automatically satisfied.

E. Statics

In the static limit, Maxwell's equation for $\vec{B}$ is

$$\vec{\nabla}\times\vec{B} = \vec{0}. \tag{20}$$

We wish to study static transverse modes. An e^{ikz} variation satisfies

$$\partial_z B_{x,y} - \partial_{x,y}B_z = ikB_{x,y} = 0,$$

with k to be determined. Since for our geometry in F2 the modes generated at the N/F2 surface should decay for increasing z, we take $\mathrm{Im}(k) > 0$.

Referring only to the spatially varying parts, we have

$$\vec{H}_\perp = -\vec{\mathcal{M}}_\perp = -\vec{M}_\perp - \vec{m}_\perp. \tag{21}$$

This ensures that there are no "magnetic poles" for $\vec{H}$ in the bulk. There are four distinct transverse components of $\vec{\mathcal{M}}$; and in general there are four distinct wave vectors k. This is necessary in order to satisfy the six N/F boundary conditions associated with $\vec{M}_\perp$ and $\vec{m}_\perp$ in F, and an $\vec{m}_\perp$ in N.

Consider how (21) affects (9). $\vec{H}_\perp = -\vec{M}_\perp - \vec{m}_\perp$ implies that, in (9), $\vec{M}_\perp$ is multiplied by $(1+\chi_\perp)$. Moreover, $\vec{m}_\perp$ is multiplied by $(-1+\lambda)$. Hence,

$$\delta\vec{M}_\perp \approx \vec{M}_\perp\left((1+\chi_\perp)+\frac{k^2}{k_A^2}\right) - \chi_\perp(\lambda-1)\vec{m}_\perp. \tag{22}$$

Now, consider how (21) affects (11). $\vec{H}_\perp = -\vec{M}_\perp - \vec{m}_\perp$ implies that $\vec{M}_\perp$ is multiplied by $(-1+\lambda)$. (References [12,23] note that the tipped exchange field $\lambda\vec{M}$ dominates over the applied field $\vec{H}$.) Moreover, $\vec{m}_\perp$ is multiplied by $(1+\chi_f)$; since $\chi_f \ll 1$, $\vec{m}_\perp$ is approximately multiplied by 1. Hence, we take

$$\delta\vec{m}_\perp \approx \vec{m}_\perp - \chi_f(\lambda-1)\vec{M}_\perp. \tag{23}$$

With $\hat{M} = \hat{z}$ we now define, for any vector $\vec{A}$, $A_+ = A_x + iA_y$, so $(\hat{M}\times\vec{A})_+ = iA_+$. We also define

$$\tilde{D}_f = D_f - i\frac{L_R}{\chi_f}, \tag{24}$$

which permits us to easily set $L_R = 0$ on replacing $\tilde{D}_f$ by D_f. Recalling the e^{ikz} spatial variation, we rewrite Eqs. (14) and (15) as

$$\partial_t M_+ = 0 = \left(i\omega_H - \frac{1}{\tau_M}\right)\delta M_+ + \frac{1}{\tau_{mM}}\delta m_+, \tag{25}$$

$$\partial_t m_+ = 0 = i\omega_X m_+ - \tilde{D}_f k^2 \delta m_+ - \frac{1}{\tau_f}\delta m_+ + \frac{1}{\tau_{Mm}}\delta M_+. \tag{26}$$

Since δM_+ explicitly depends on k^2, in what follows we employ M_+ and m_+.

We now multiply (25) by τ_M and (26) by τ_f. Then, using (22) and (23), and the previously cited relation $\omega_H\tau_M = \alpha$, we obtain a form with dimensionless coefficients

$$0 = M_+\left[\left(\frac{i}{\alpha}-1\right)\left(1+\chi_\perp+\frac{k^2}{k_A^2}\right) - \frac{(\lambda-1)\chi_f\tau_M}{\tau_{mM}}\right] + m_+\left[-(\lambda-1)\chi_\perp\left(\frac{i}{\alpha}-1\right)+\frac{\tau_M}{\tau_{mM}}\right], \tag{27}$$

$$0 = m_+\left[i\omega_X\tau_f - (\tilde{D}_f\tau_f k^2+1) - \frac{(\lambda-1)\chi_\perp\tau_f}{\tau_{Mm}}\right] + M_+\left[(\lambda-1)\chi_f(\tilde{D}_f\tau_f k^2+1) + \frac{\left(1+\chi_\perp+\frac{k^2}{k_A^2}\right)\tau_f}{\tau_{Mm}}\right]. \tag{28}$$

The -1 in $\lambda-1$ appears because of the demagnetization fields that $\vec{M}_\perp$ and $\vec{m}_\perp$ exert on one another.

F. Statics with no cross decay and $L_R = 0$

For simplicity we now set the spin accumulation stiffness $L_R = 0$ (so $\tilde{D}_f \to D_f$), and we neglect cross decay ($\tau_{mM}, \tau_{Mm} \to \infty$). One result of this is that α disappears from the equations. Moreover, (27) gives

$$\frac{m_+}{M_+} = \frac{1+\chi_\perp+\frac{k^2}{k_A^2}}{(\lambda-1)\chi_\perp}. \tag{29}$$

Solving Eqs. (27) and (28) for k^2 gives a quadratic equation in k^2, which we write in terms of $(k/k_A)^2$ with dimensionless coefficients

$$\left(\frac{k}{k_A}\right)^4 + b\left(\frac{k}{k_A}\right)^2 + c = 0, \tag{30}$$

where

$$b = \left[(1+\chi_\perp) - \frac{(i\omega_X\tau_f - 1) - (\lambda-1)^2\chi_\perp\chi_f}{D_f\tau_f k_A^2}\right], \tag{31}$$

$$c = -\frac{1}{D_f\tau_f k_A^2}[(1+\chi_\perp)(i\omega_X\tau_f - 1) + (\lambda-1)^2\chi_\perp\chi_f]. \tag{32}$$

The (complex) solutions are given by

$$k^2 = \tfrac{1}{2}(-b \pm \sqrt{b^2-4c}). \tag{33}$$

V. MATERIAL PARAMETERS

To determine the mode wave vectors requires a number of material parameters, given for one conducting magnet (permalloy, or Py) and one insulating magnet (yttrium iron garnet, or YIG) in Table I. These values are largely taken from Ref. [38]. However, a number of material parameters come from other sources or from estimates. For YIG we take two values of λ. The value $\lambda = 225$ is obtained from $\lambda = T_c/C$, where C is the Curie constant given by $C = \mu_0 n\mu_B^2 g^2 S(S+1)/(3k_B)$, where $n = 1.06\times10^{27}$ m^{-3} is the number density of spins, $g = 2$ is the g factor, and $S = 14.5$ is the spin per

TABLE I. Parameters for Py and YIG used in calculations, mostly from Ref. [38]. Two exchange-related constants appear. λ is the dimensionless uniform exchange constant that determines the mean-field transition temperature (because of the uncertainty in its value for YIG, we employ the same two values for YIG and Py). A is the exchange constant associated with nonuniformity of the magnetization. In figures where λ is varied, λ also is varied in ω_X. For many figures, H takes on different values.

Quantity	Py	YIG
M (A/m)	8.6×10^5	1.42×10^5
γ (Hz/T)	1.847×10^{11}	1.847×10^{11}
λ	500, 3300	500, 3300
A (J/m)	1.3×10^{-11}	3.65×10^{-12}
D_f (m^2/s)	1.0×10^{-3}	5.0×10^{-3}
α	0.005	0.0006
$\tau_{ML} \approx \tau_M = (\alpha\omega_H)^{-1}$ (s)	3×10^{-10}	1×10^{-2}
$\tau_{mL} \approx \tau_f$ (s)	3×10^{-14}	1×10^{-6}
$l_L = \sqrt{D_f\tau_f}$ (m)	5.5×10^{-9}	7.1×10^{-5}

unit cell. Because $\lambda = 225$ gives a rather low value for ω_X, for calculations we consider $\lambda = 500$ and 3300, the value for Py.

For transverse diffusion and decay we assume that diffusion and decay of excitations is the same for both longitudinal and transverse excitations, where the diffusion longitudinal length is defined as

$$l_L \equiv \sqrt{D_f \tau_f} \approx \sqrt{D_f \tau_{mL}}. \tag{34}$$

For YIG, we take D_f from Ref. [42] and we take τ_f from Ref. [35]. This appears only in the dimensionless product $(k_A l_F)^2$, of which each part is reasonably well known. Likewise, the dimensionless quantity $\omega_X \tau_f$ that appears is reasonably well known, as is $\chi_\perp$. Less well known is χ_f, due to the excitations.

The next section numerically evaluates the mode eigenvalues (wave vectors) and eigenvectors for both Py and YIG, exploring how they vary with λ. Unlike quantum mechanics where there is mode crossing for a fixed off-diagonal parameter V at varying energies E_1 and E_2, in the present case the parameter λ varies both off diagonal and on diagonal. This complicates the interpretation considerably. The Appendix explores how the k's vary with the largely unknown mutual decay rate τ_{Mm}.

VI. INTERPRETING THE NUMERICS

The theory is surprisingly complex to interpret. One reason is that because the theory yields equations that are non-Hermitian, the normal modes are not orthogonal, and thus it is especially important to study the eigenfunctions of the normal modes, as well as the normal modes (the wave vectors).

Another reason is that the theory involves three parameters that are not precisely known. These parameters, from most to least well known, are (1) the exchange parameter λ; (2) the transverse susceptibility of the excitations χ_f; and (3) the decay time τ_{mM}. χ_f may be close to the longitudinal susceptibility of the excitations, which by definition is the usual longitudinal susceptibility χ_l. τ_{mM} and τ_{mM} are related by an Onsager relation involving $\chi_\perp$ and χ_f, and are new to theories of ferromagnetic response in modern spintronics. (However, as noted earlier, they have their origins in Hasegawa's *s-d* model for Mn in Cu [24].)

Our strategy to study the parameter dependence of the two mode structures m_+/M_+ and the two eigenmodes k is as follows. (1) We relegate the dependence on τ_{mM} to the Appendix; (2) we display the dependence on χ_f for a large range of χ_f using a logarithmic plot for the m_+/M_+'s and a semilogarithmic plot for the k's; and (3) we explore the dependence on λ for the two plausible values 3300 (solid lines) and 500 (dashed lines); (4) we consider three experimentally accessible values for $\mu_0 H$: 0.1, 1.0, and 10.0 T. We employ circles for $\lambda = 3300$ and triangles for $\lambda = 500$, with increasing size to denote increasing field.

For each mode, m_+/M_+ and k are complex. As a consequence, each mode contributes a decaying and an oscillating part. To be specific, the transverse decay lengths are defined, for modes $n = 1, 2$, via

$$l_{Tn} = \frac{1}{\mathrm{Im}\{k_n\}}, \tag{35}$$

and the transverse wavelengths are defined by

$$\lambda_{Tn} = \frac{2\pi}{\mathrm{Re}\{k_n\}}. \tag{36}$$

Hence, if a sample can be made of varying thickness d but of such regularity that the boundary conditions are the same at both surfaces, in comparing the dependence on d one must employ two decay lengths and two wavelengths.

Although spintronics first involved studies of conducting ferromagnets, such as permalloy (Py), because of the longer longitudinal decay length (from spin flip and diffusion) of magnetic insulators like YIG, more recent work has focused on materials like YIG [43]. For that reason, we first study the properties of YIG. Note that YIG has a complex structure with three inequivalent magnetic lattices, and although at room temperatures they are collinear, at low temperatures they are noncollinear. This noncollinearity is an early example of competing interactions; it results in a low-temperature noncollinear phase [44]. Here, the noncollinear order "melts" as the temperature increases, not unlike what has been posited for the appearance of spin-glass order at low temperatures in magnetic alloys known as reentrant spin glasses [45].

VII. EIGENMODES AND EIGENWAVE VECTORS FOR YIG

For YIG we now show our results for the eigenmodes and the eigenvectors. Although the mode ratios m_+/M_+ are complex, with the phase relationship a measurable quantity, we present only $|m_+/M_+|$. We do this before presenting the normal modes k_n in order to facilitate interpretation of the modes.

Figure 2(a) shows that for mode 1, m_+/M_+ is always dominated by M_+. Also, the dependence on λ involves a crossover, depending on the value of χ_f. Further, m_+/M_+ increases as H increases. We may think of this as a mostly M mode.

Figure 2(b) shows that mode 2 is more complex: for $\chi_f < 10^{-4}$ m_+/M_+ is dominated by M_+, increasing λ decreases m_+/M_+, and increasing H increases m_+/M_+. However, for $\chi_f > 10^{-3}$ m_+/M_+ is dominated by m_+, increasing λ increases m_+/M_+, and increasing H has little effect on m_+/M_+. For large enough χ_f we may think of this as a mostly m mode.

The corresponding eigenvalues are given in Figs. 3 and 4. We take the imaginary parts to be positive. Figure 3(a) shows that $\mathrm{Re}(k_1)$ vs χ_f has a resonancelike shape. With increasing λ the peak position in $\mathrm{Re}(k_1)$ decreases but its peak value increases. With increasing H, both its peak position and peak value increase. Figure 3(b) shows that $\mathrm{Im}(k_1)$ vs χ_f rolls over to zero for increasing χ_f, for all λ and H. With increasing λ the peak position in $\mathrm{Im}(k_1)$ decreases but its peak value increases. With increasing H, both its peak position and peak value increase. Figure 4(a) shows that $\mathrm{Re}(k_2)$ is nearly independent of H, and increases with increasing λ. $\mathrm{Re}(k_2)$ is very small for small χ_f, corresponding to a very long spatial period of oscillation. However, for increasing χ_f, $\mathrm{Re}(k_2)$ grows to values that correspond to a very short spatial period. Figure 4(b) shows that $\mathrm{Im}(k_2)$ vs χ_f has a constant small χ_f value that is independent of H but increases as λ increases. For $\mu_0 H = 10$ T, as χ_f increases $\mathrm{Im}(k_2)$ goes to a peak and then falls to zero. For smaller H, as χ_f increases $\mathrm{Im}(k_2)$ simply rolls over to zero.

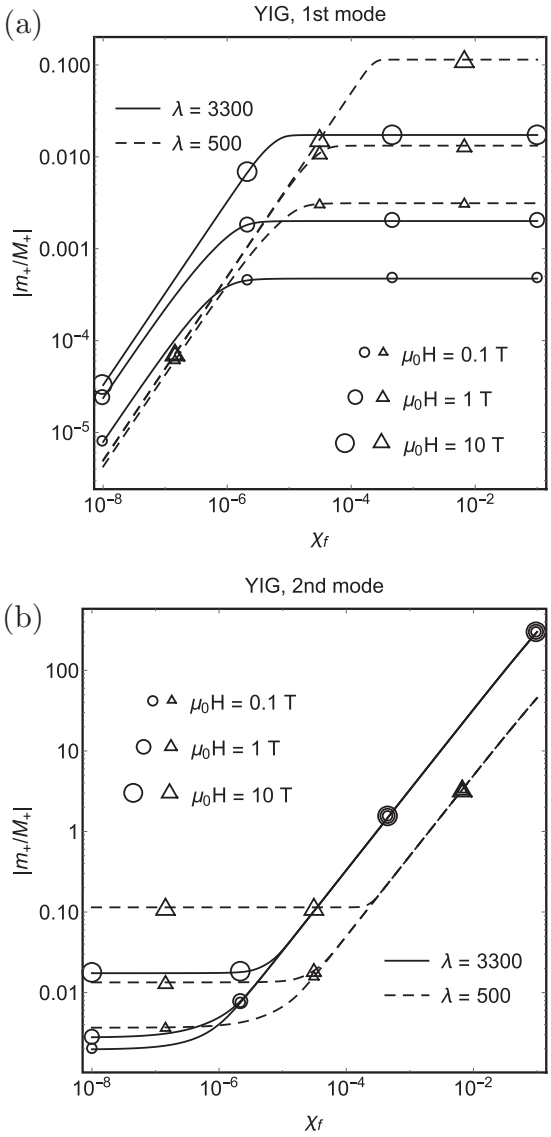

FIG. 2. For YIG, the eigenmode ratios $|m_+/M_+|$ parametrized by λ and $\mu_0 H$ for no mutual decay: (a) k_1; (b) k_2. Solid lines indicate $\lambda = 3300$, with circles of increasing size indicating large $\mu_0 H$. Dashed lines indicates $\lambda = 500$, with triangles of increasing size indicating large $\mu_0 H$. Both vertical and horizontal scales are dimensionless.

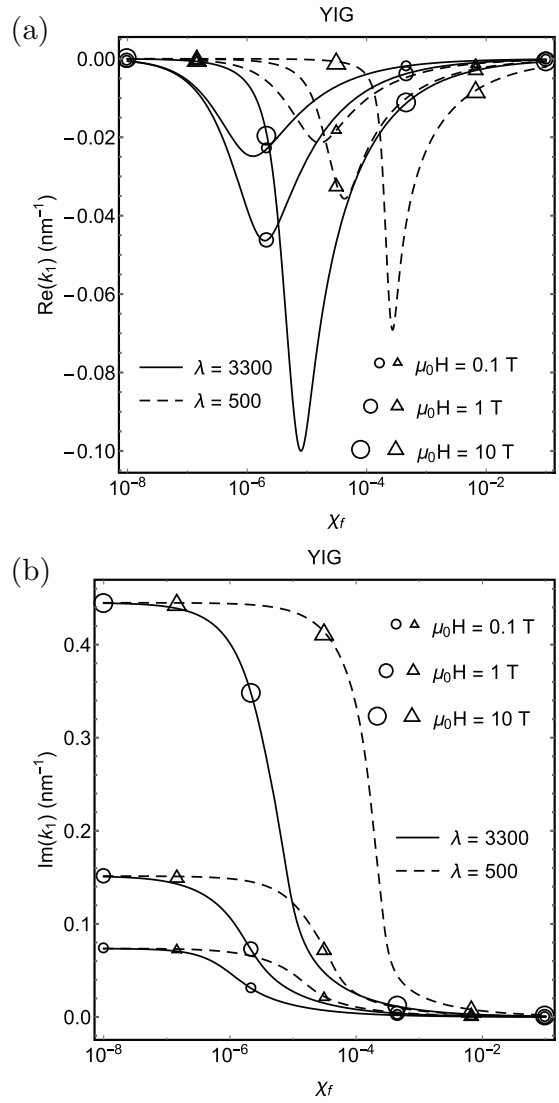

FIG. 3. For YIG the eigenvalues k_1 vs λ with no mutual decay: (a) $\mathrm{Re}(k_1)$; (b) $\mathrm{Im}(k_1)$. The vertical scales are in nm^{-1} and the horizontal scales are dimensionless.

VIII. EIGENMODES AND EIGENWAVE VECTORS FOR PY

In the absence of a detailed knowledge of λ for Py, we employ the same values 3300 and 500 as for YIG. For Py we now show our results for the eigenmodes and the eigenvectors. Although the mode ratios m_+/M_+ are complex, with the phase relationship a measurable quantity, we present only $|m_+/M_+|$. As for YIG we do this before presenting the normal modes k_n in order to facilitate interpretation of the modes. In general, the results are very similar qualitatively to those for YIG, but they differ in detail.

Figure 5(a) shows that for mode 1, m_+/M_+ is always dominated by M_+. Also, the dependence on λ involves a crossover, depending on the value of χ_f. Further, m_+/M_+ increases as H increases. We may think of this as a mostly M mode. Figure 5(b) shows that mode 2 is more complex: for $\chi_f < 10^{-4}$ m_+/M_+ is dominated by M_+, increasing λ decreases m_+/M_+, and increasing H increases m_+/M_+. However, for $\chi_f > 10^{-3}$ m_+/M_+ is dominated by m_+, increasing λ increases m_+/M_+, and increasing H has little effect on m_+/M_+. For large enough χ_f, we may think of this as a mostly m mode.

The corresponding eigenvalues are given in Figs. 6 and 7. Our convention is that imaginary parts are taken to be positive. Figure 6(a) shows that $\mathrm{Re}(k_1)$ vs χ_f has a resonancelike shape. With increasing λ, the peak position in $\mathrm{Re}(k_1)$ decreases but its peak value increases. With increasing H, both its peak position and peak value increase. Figure 6(b) shows that $\mathrm{Im}(k_1)$ vs χ_f rolls over to zero for increasing χ_f, for all λ and H. With increasing λ the peak position in $\mathrm{Im}(k_1)$ decreases but its peak value increases. With increasing H, both its peak position and peak value increase. The $\lambda = 500$, $\mu_0 H = 0.1$ T peak is much lower than for YIG. Figure 7(a) shows that $\mathrm{Re}(k_2)$ is nearly independent of H, and increases with increasing λ.

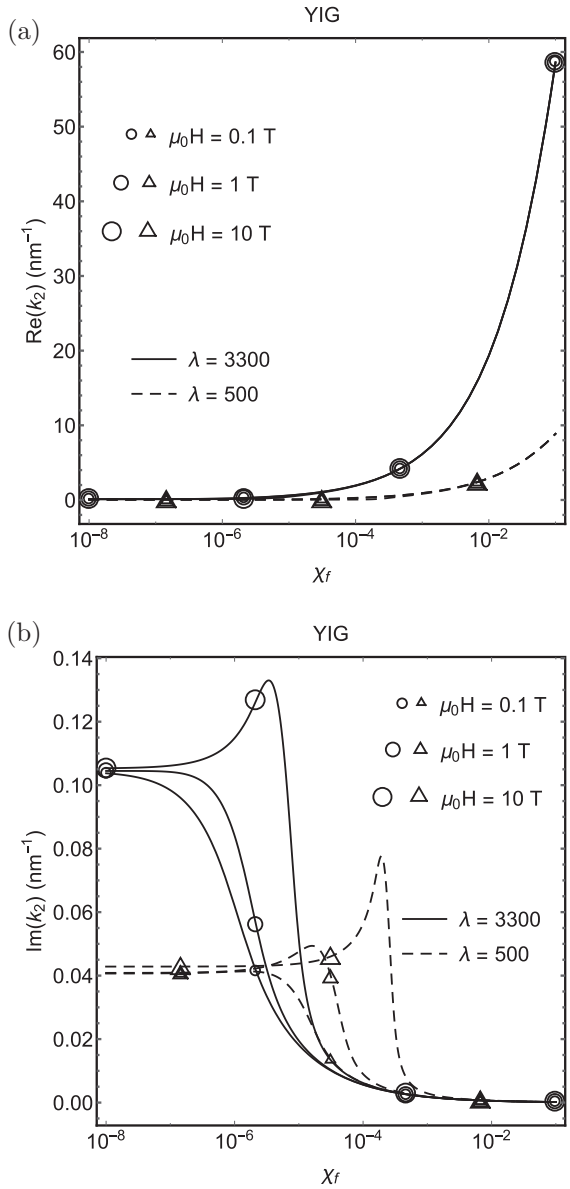

FIG. 4. For YIG the eigenvalues k_2 vs λ with no mutual decay: (a) Re(k_2); (b) Im(k_2). The vertical scales are in nm^{-1} and the horizontal scales are dimensionless.

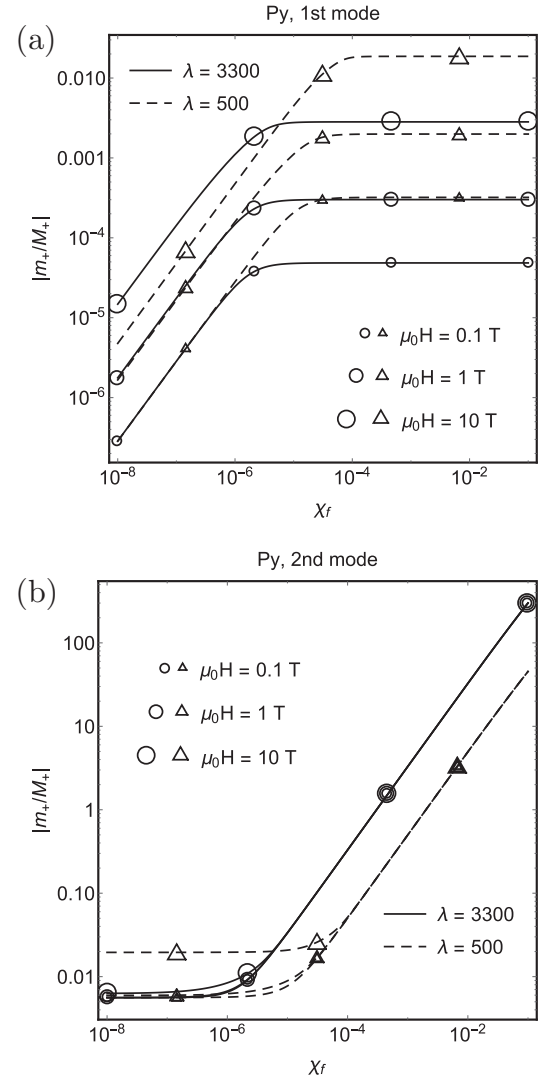

FIG. 5. For Py, the eigenmode ratios $|m_+/M_+|$ parametrized by λ and $\mu_0 H$ for no mutual decay: (a) k_1; (b) k_2. Solid lines indicate $\lambda = 3300$, with circles of increasing size indicating large $\mu_0 H$. Dashed lines indicates $\lambda = 500$, with triangles of increasing size indicating large $\mu_0 H$. Both vertical and horizontal scales are dimensionless.

Re(k_2) is very small for small χ_f, corresponding to a very long spatial period of oscillation. For increasing χ_f, Re(k_2) grows to values that correspond to a very short spatial period. Figure 7(b) shows that Im(k_2) vs χ_f has a small constant value, independent of H, but increases as χ_f increases. As χ_f increases, for $\lambda = 500$ and $\mu_0 H = 10$ T, Im(k_2) goes to a (small) peak and then falls to zero. For smaller H, Im(k_2) rolls over to zero. For $\lambda = 3300$ and all three H, Im(k_2) rolls over to zero.

IX. EXPERIMENTAL CONSIDERATIONS

We now consider two dc spin current experiments for which the values of the longitudinal and transverse decay lengths relative to sample thicknesses are relevant.

A. Spin transfer in conductors

Shortly after Slonczewski's proposal of spin transfer [8], experiments using large applied currents established both spin transfer and, for strong applied fields, spin-wave generation [11]. Reference [11] used a multilayer of Co(10 nm)/Cu(6 nm)/Co(2.5 nm). Assuming that Co has properties similar to those of Py, such a $d = 6$ nm sample thickness is near the transverse decay length 7.1 nm of mode 1, but much larger than the transverse decay length 2.4 nm of mode 2. Therefore, although our above estimates for Py indicate that mode 2 decays significantly for $d = 6$ nm, mode 1 does not decay significantly within that distance, so that all of the spin that is transferred at the interface does not decay to the lattice, and it can tip the net $\vec{M}$, as observed for large amplitude currents.

For thicker samples and small currents, the net $\vec{M}$ would not appear to be tipped. We thus expect that, for sample

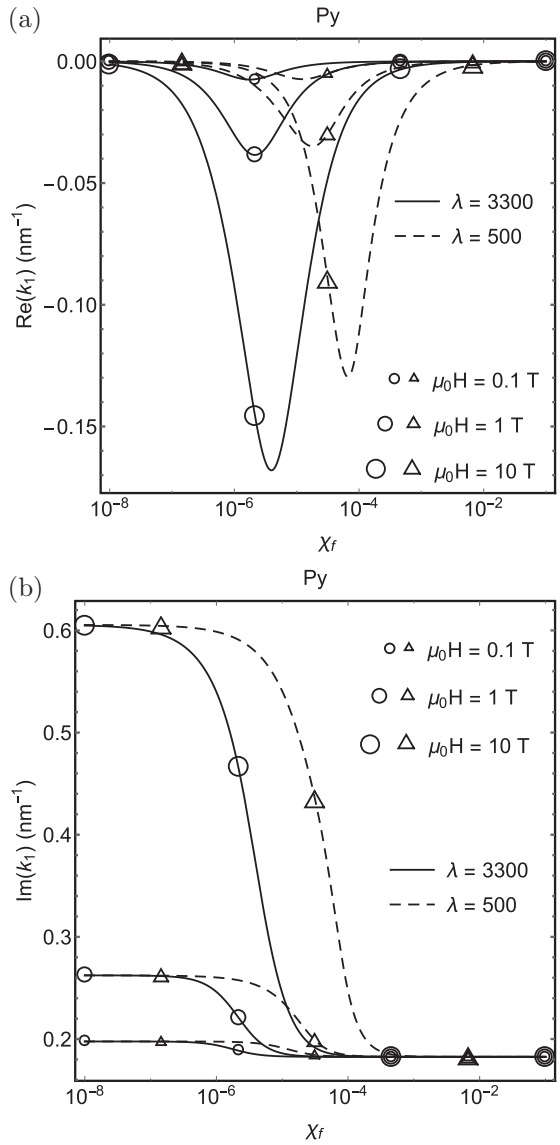

FIG. 6. For Py the eigenvalues k_1 vs λ with no mutual decay: (a) Re(k_1); (b) Im(k_1). The vertical scales are in nm^{-1} and the horizontal scales are dimensionless.

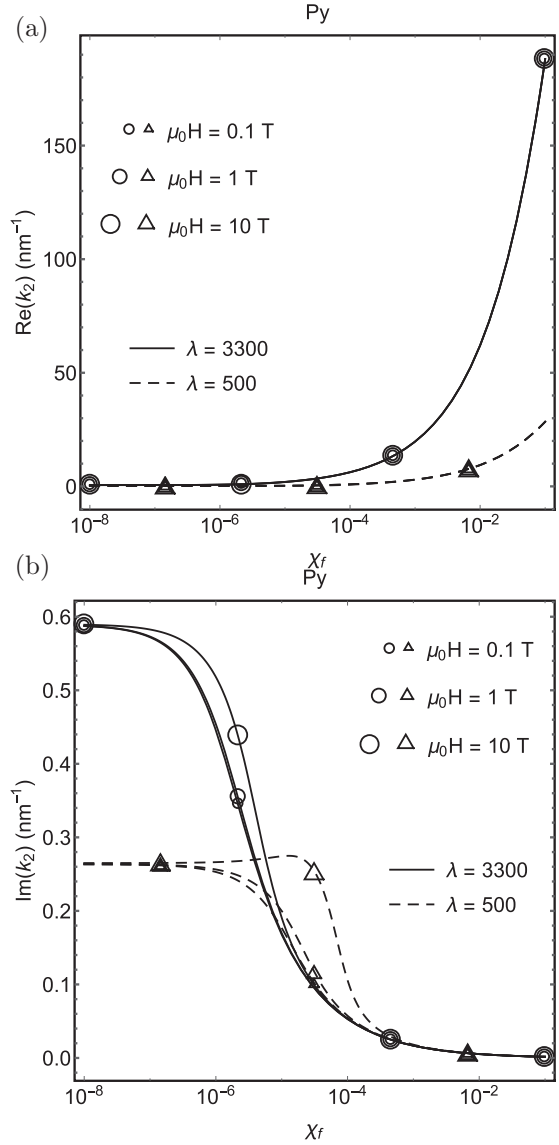

FIG. 7. For Py the eigenvalues k_2 vs λ with no mutual decay: (a) Re(k_2); (b) Im(k_2). The vertical scales are in nm^{-1} and the horizontal scales are dimensionless.

thicknesses exceeding both transverse decay lengths, spin transfer will be more difficult to observe. For comparison, Ref. [46] gives a room-temperature longitudinal decay length for Co of 140 nm.

Note that Ref. [47] gives, for the alloy permalloy (Py) at room temperature, a much shorter 3-nm longitudinal decay length. Reference [48] gives a useful and general experimental review, for metals and alloys, of spin-diffusion lengths and of spin flip at metal/metal interfaces.

To summarize, if the three decay lengths satisfy $l_{T2} \ll l_{T1} \ll l_L$, then there are four regimes of longitudinal and transverse behavior as a function of film thickness d, according to which of the modes decay and which remain over the distance d. Moreover, because these modes have complex wave vectors, there will be oscillations in addition to decay, thus complicating the interpretation.

B. "Magnon-mediated" current drag in insulators

An effect called "magnon drag" was proposed by Zhang and Zhang [14]. Consider a multilayer where spin-orbit active normal metals NM sandwich a ferromagnet F (conductor or insulator). By the spin Hall effect in NM1, a charge current along the NM1 layer drives a spin current through F to NM2 (which could be the same as NM1), where by the inverse spin Hall effect a charge current entering NM2 is generated along the surface of NM2. The effect was predicted for the spin-polarization direction of the spin current along the magnetization in F, a *longitudinal* effect.

The effect indeed was observed for the insulator YIG for thicknesses that likely were short compared to the longitudinal spin decay length, but long compared to the transverse decay lengths [15–17]. There, we expect the effect can be observed only for longitudinal magnetization. However, for thinner

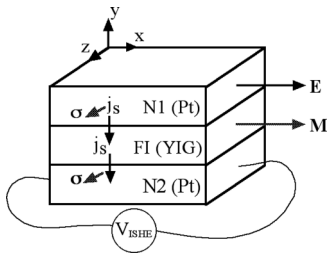

FIG. 8. Proposed transverse "'magnon drag" experiment. The spin current is j_s along $-y$, and the polarization of the spin current in the FI is denoted by σ, as is conventional in such experiments.

samples, the effect for transverse magnetization should also occur.

Specifically, Ref. [15] used YIG thicknesses <5 μm and for 3–50 μm; in addition to observing the predicted effect, they found a longitudinal decay length of about 9 μm. Reference [49] gives a longitudinal decay length at room temperature for YIG of 10 μm. Reference [16] used the relatively small YIG thickness of about 8 nm, and Ref. [17] used the relatively large YIG thicknesses of 40, 60, 80, and 100 μm. Given the uncertainty in χ_f, it is not clear what the theory predicts for the decay lengths of the modes; see Figs. 3(b) and 4(b).

In addition to the longitudinal magnon drag effect, for sample thicknesses that do not exceed the transverse decay lengths, the present theory indicates that there should be a transverse magnon drag effect, indicated in Fig. 8. By the spin Hall effect an applied $\vec{E}$ in top layer N1 drives a spin Hall current j_s, spin polarized with $\vec{\sigma} \equiv \vec{m}$ along z, into the insulating F1, whose $\vec{M}$ is along x. Hence, the spin current is transverse to $\vec{M}$. By bulk irreversible thermodynamics, if the sample is thinner than the transverse decay lengths, which from Figs. 3(b) and 4(b) we estimate to be of order 2–10 nm, then the spin current will reach the FI/N2 interface. By surface irreversible thermodynamics, a spin current then will be

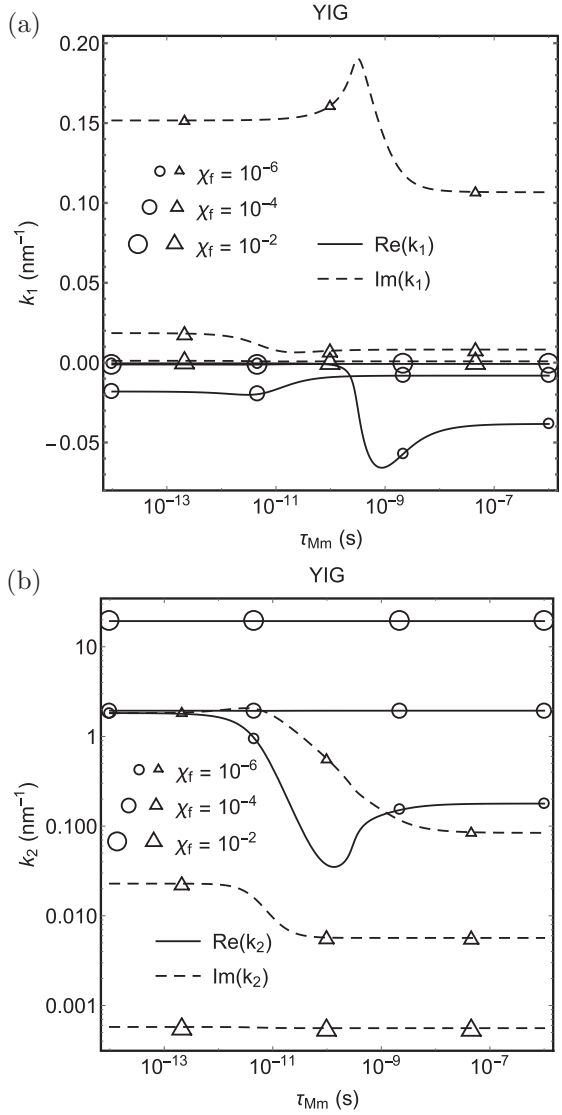

FIG. 9. For YIG, the eigenvalues k vs τ_{Mm} for mutual decay with $\lambda = 3300$ and three values for χ_f: (a) k_1; (b) k_2.

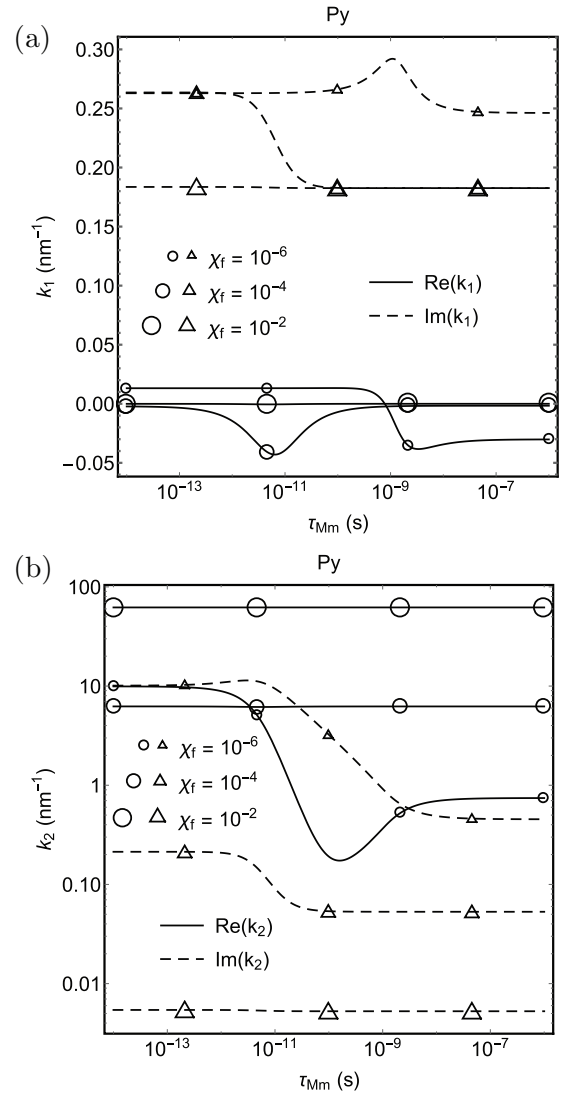

FIG. 10. For Py, the eigenvalues k vs τ_{Mm} for mutual decay with $\lambda = 3300$ and three values for χ_f: (a) k_1; (b) k_2.

"pumped" across the FI/N2 interface (spin convertance). For this dc case, "coherent" $\vec{M} \times d\vec{M}/dt$ based theories predict zero spin transfer current j_s from F to N2.

X. IMPLICATIONS

This work shows that, except perhaps for very small sample thicknesses, the response of a ferromagnet to a transverse spin current does not simply consist of a redefined axis for the magnetization. A recently studied ferromagnetic insulator (FI) might provide a useful example. We refer to a study of the spin Seebeck effect (temperature gradient producing a spin current) and spin transfer torque by magnons [50]. This work considers a FI/AF/FI sandwich subject to gradients in both temperature and longitudinal spin chemical potential. When the system thicknesses do not exceed the transverse decay lengths discussed in this work, the transverse response should be nontrivial. For such very short lengths, the theory provides the appropriate number of parameters to interpret experiments, even if the associated parameter values are not known accurately.

We have not discussed an example of a semiconducting magnet, where the length scales for both longitudinal and transverse modes may be intermediate between the values for conductors and insulators. Again, both transverse modes are likely to be essential to describing the transverse response.

XI. SUMMARY AND CONCLUSIONS

We have studied the small-amplitude static transverse modes of ferromagnets, both conducting and insulating. There are four coupled transverse degrees of freedom and the corresponding modes, which are excited according to the boundary conditions. For the spin accumulation $\vec{m}$, these are spin currents across the interface both conserved and proportional to the difference across the interface in the spin chemical potential, and for the magnetization $\vec{M}$ these are the usual micromagnetic boundary conditions, which may include an exchange coupling between adjacent materials.

This transverse response has broad implications for spintronics at the nanoscale. There, even for conducting magnets, the system dimensions can be small enough that the transverse mode characteristic lengths are long enough that their effect cannot be interpreted as a phenomenon that occurs almost immediately at the surface.

ACKNOWLEDGMENTS

We would like to thank M. Stiles and T. Taniguchi for valuable and informative conversations.

APPENDIX

Use of (27) and (28) permits us to include the effect of the mean-field exchange constant λ and of the cross decay τ_{mM} on the real and imaginary parts of the wave vectors. What follows is only exploratory, and therefore considers only the case $\lambda = 3300$ and $\mu_0 H = 1$ T. Figure 9 plots, for YIG with $\chi_f = 10^{-2},\ 10^{-4},\ 10^{-6}$ the eigenvalues k vs τ_{Mm}. Unfortunately, we know of no current experiments that yield a value for τ_{Mm}.

Figure 10 plots, for Py with $\chi_f = 10^{-2},\ 10^{-4},\ 10^{-6}$ the eigenvalues k vs τ_{Mm}. The limit of negligible cross decay is $\tau_{Mm} \to \infty$. Unfortunately, we know of no current experiments that yield a value for τ_{Mm}.

[1] M. Johnson and R. H. Silsbee, Phys. Rev. B **35**, 4959 (1987).
[2] The term *evanescent* waves refers to modes at a surface, usually with relatively little damping, as when light within insulator A is incident on insulator B at an angle that exceeds the critical angle, and decays exponentially within B with negligible energy loss. Also called *surface modes*, they may have considerable damping; nevertheless, some might prefer the term evanescent waves even when, as in the case of the spin-flip-diffusion mode of Ref. [1], there is no oscillation at all.
[3] A. G. Aronov, Pisma Zh. Eksp. Teor. Fiz. **24**, 37 (1976) [JETP Lett. **24**, 32 (1976)].
[4] P. C. van Son, H. van Kempen, and P. Wyder, Phys. Rev. Lett. **58**, 2271 (1987).
[5] T. Valet and A. Fert, Phys. Rev. B **48**, 7099 (1993).
[6] M. N. Baibich, J. M. Broto, A. Fert, F. Nguyen Van Dau, F. Petroff, P. Eitenne, G. Creuzet, A. Friederich, and J. Chazelas, Phys. Rev. Lett. **61**, 2472 (1988).
[7] G. Binasch, P. Grünberg, F. Saurenbach, and W. Zinn, Phys. Rev. B **39**, 4828 (1989).
[8] J. C. Slonczewski, J. Magn. Magn. Mater. **159**, L1 (1996).
[9] P. Grünberg, R. Schreiber, Y. Pang, M. B. Brodsky, and H. Sowers, Phys. Rev. Lett. **57**, 2442 (1986).
[10] E. B. Myers, D. C. Ralph, J. A. Katine, R. N. Louie, and R. A. Buhrman, Science **285**, 867 (1999).
[11] J. A. Katine, F. J. Albert, R. A. Buhrman, E. B. Myers, and D. C. Ralph, Phys. Rev. Lett. **84**, 3149 (2000).
[12] R. H. Silsbee, A. Janossy, and P. Monod, Phys. Rev. B **19**, 4382 (1979); In this work the driving term for the interfacial spin current includes a term $A_1' d\hat{M}$, so that for $\hat{M}$ along $\hat{z}$ the x component is $A_1' d\hat{M}_x$. The authors note that the measured phase of their signal precludes a driving term of the form $A_2' \vec{M} \times d\hat{M}$.
[13] W. M. Saslow, Phys. Rev. B **95**, 184407 (2017); Appendix A treats magnetic insulators.
[14] S. S.-L. Zhang and S. Zhang, Phys. Rev. Lett. **109**, 096603 (2012).
[15] L. J. Cornelissen, J. Liu, R. A. Duine, J. Ben Youssef, and B. J. van Wees, Nat. Phys. **11**, 1022 (2015).
[16] J. Li, Y. Xu, M. Aldosary, C. Tang, Z. Lin, S. Zhang, R. Lake, and J. Shi, Nat. Commun. **7**, 10858 (2016).
[17] H. Wu, C. H. Wan, X. Zhang, Z. H. Yuan, Q. T. Zhang, J. Y. Qin, H. X. Wei, X. F. Han, and S. Zhang, Phys. Rev. B **93**, 060403(R) (2016).
[18] T. Taniguchi and W. M. Saslow, Phys. Rev. B **90**, 214407 (2014).
[19] D. Qu, S. Y. Huang, J. Hu, R. Wu, and C. L. Chien, Phys. Rev. Lett. **110**, 067206 (2013).
[20] D. Yue, W. Lin, J. Li, X. Jin, and C. L. Chien, Phys. Rev. Lett. **121**, 037201 (2018).

[21] A. Brataas, Y. V. Nazarov, and G. E. W. Bauer, Eur. Phys. J. B **22**, 99 (2001).
[22] M. D. Stiles and A. Zangwill, Phys. Rev. B **66**, 014407 (2002).
[23] S. Zhang, P. M. Levy, and A. Fert, Phys. Rev. Lett. **88**, 236601 (2002).
[24] H. Hasegawa, Prog. Theor. Phys. **21**, 483 (1959).
[25] S. Schultz, D. R. Fredkin, B. L. Gehman, and M. R. Shanabarger, Phys. Rev. Lett. **31**, 1297 (1973).
[26] Y. Tserkovnyak, A. Brataas, and G. E. W. Bauer, Phys. Rev. Lett. **88**, 117601 (2002); In this work the driving term for interfacial spin current varies as $A_1\hat{M}\times d\vec{M}/dt + A_2\hat{M}\times(\hat{M}\times d\vec{M}/dt)$, so that for $\hat{M}$ along $\hat{z}$ the x component is $A_1(dM_y/dt) - A_2(dM_x/dt)$.
[27] L. D. Flesner, D. R. Fredkin, and S. Schultz, Solid State Commun. **18**, 207 (1976).
[28] J. Zhang, P. M. Levy, S. Zhang, and V. Antropov, Phys. Rev. Lett. **93**, 256602 (2004).
[29] Y. Tserkovnyak, A. Brataas, and G. E. W. Bauer, J. Appl. Phys. **93**, 7534 (2003).
[30] K. M. Schep, J. B. A. N. van Hoof, P. J. Kelly, G. E. W. Bauer, and J. E. Inglesfield, J. Magn. Magn. Mater. **177**, 1166 (1998); Phys. Rev. B **56**, 10805 (1997);
[31] D. R. Penn and M. D. Stiles, Phys. Rev. B **59**, 13338 (1999).
[32] M. D. Stiles and D. R. Penn, Phys. Rev. B **61**, 3200 (2000).
[33] Y. Tserkovnyak, A. Brataas, and G. E. W. Bauer, Phys. Rev. B **66**, 224403 (2002).
[34] I. M. Khalatnikov, Zh. Eksp. Teor. Fiz. **22**, 687 (1952); See also Chapter 23 of *Introduction to the Theory of Superfluldity* (Benjamin, New York, 1965).
[35] S. S.-L. Zhang and S. Zhang, Phys. Rev. B **86**, 214424 (2012).
[36] G. T. Rado and J. R. Weertman, Phys. Rev. **94**, 1386 (1954).
[37] W. S. Ament and G. T. Rado, Phys. Rev. **97**, 1558 (1955).
[38] C. Sun and W. M. Saslow, Phys. Rev. B **97**, 174411 (2018).
[39] D. C. Langreth, D. L. Cowan, and J. W. Wilkins, Solid State Commun. **6**, 131 (1968).
[40] D. C. Langreth and J. W. Wilkins, Phys. Rev. B **6**, 3189 (1972).
[41] M. B. Walker, Phys. Rev. B **1**, 3690 (1970).
[42] B. L. Giles, Z. Yang, J. S. Jamison, and R. C. Myers, Phys. Rev. B **92**, 224415 (2015).
[43] M. Althammer, J. Phys. D: Appl. Phys. **51**, 313001 (2018).
[44] A. E. Clark and E. Callen, J. Appl. Phys. **39**, 5972 (1968); These authors consider a two-sublattice model with competing interactions.
[45] W. M. Saslow and G. Parker, Phys. Rev. Lett. **56**, 1074 (1986); These authors model spin-glass sites within a ferromagnet.
[46] L. Piraux, S. Dubois, A. Fert, and L. Belliard, Eur. Phys. J. B **4**, 413 (1998).
[47] E. Sagasta, Y. Omori, M. Isasa, Y.-C. Otani, L. E. Hueso, and F. Casanova, Appl. Phys. Lett. **111**, 082407 (2017).
[48] J. Bass and W. P. Pratt, J. Phys.: Condens. Matter **19**, 183201 (2007).
[49] L. J. Cornelissen and B. J. van Wees, Phys. Rev. B **93**, 020403(R) (2016).
[50] Y. Cheng, K. Chen, and S. Zhang, Appl. Phys. Lett. **112**, 052405 (2018).